Nuclear Materials and Energy 15 (2018) 64–70

Contents lists available at ScienceDirect

Nuclear Materials and Energy

journal homepage: www.elsevier.com/locate/nme

Linear scaling DFT calculations for large tungsten systems using an optimized local basis

Stephan Mohr[*,a], Marc Eixarch[a], Maximilian Amsler[b], Mervi J. Mantsinen[a,c], Luigi Genovese[d,e]

[a] Barcelona Supercomputing Center (BSC), C/ Jordi Girona 29, Barcelona 08034, Spain
[b] Laboratory of Atomic and Solid State Physics, Cornell University, Ithaca, New York 14853, USA
[c] ICREA, Pg. Lluís Companys 23, Barcelona 08010, Spain
[d] Univ. Grenoble Alpes, INAC-MEM, L_Sim, Grenoble,F-38000, France
[e] CEA, INAC-MEM, L_Sim, Grenoble F-38000, France

ABSTRACT

Density functional theory (DFT) has become a standard tool for ab-initio simulations for a wide range of applications. While the intrinsic cubic scaling of DFT was for a long time limiting the accessible system size to some hundred atoms, the recent progress with respect to linear scaling DFT methods has allowed to tackle problems that are larger by many orders of magnitudes. However, as these linear scaling methods were developed for insulators, they cannot, in general, be straightforwardly applied to metals, as a finite (electronic) temperature is needed to ensure locality of the density matrix. In this paper we show that, once finite electronic temperature is employed, the linear scaling version of the BIGDFT code is able to exploit this locality to provide a computational treatment that scales linearly with respect to the number of atoms of a metallic system. We provide prototype examples based on bulk Tungsten, which plays a key role in finding safe and long-lasting materials for Fusion Reactors; however we do not expect any major obstacles in extending this work to cover other metals. We believe that such an approach might help in opening the path towards novel approaches for investigating the electronic structure of such materials, in particular when large supercells are required.

1. Introduction

One of the big challenges towards the use of Fusion as a source of clean and safe energy is the design of appropriate reactor components. During the past years, Tungsten-based materials have emerged as very promising candidates, thanks to their high melting point, high thermal conductivity, low coefficient of thermal expansion, high sputtering threshold energy, low tritium retention and low neutron activation [1]. These materials will sustain high radiation levels which will produce defects that alter their mechanical and transport properties. Understanding the nature of these defects, such as their atomic structure as well as electronic and magnetic properties, is fundamental to build predictive models of microstructure evolution under irradiation. In this quest, first principles calculations have been crucial to elucidate the properties and characteristics of the smallest defects, single self-interstitials and vacancies [2,3]. But up to now, only clusters with just a few defects can be studied with these methods.

Over the past decades Kohn–Sham (KS) density functional theory [4,5] (DFT) has become the most popular method for first principles quantum mechanical calculations thanks to the good balance between precision and efficiency offered by this approach. In particular, DFT offers a much better scaling with respect to the system size compared to other ab-initio approaches. More precisely, the computational cost scales as the third power of the number of Kohn–Sham orbitals, i.e. it is $\mathcal{O}(N^3)$.

Nevertheless, this inherent cubic scaling still limits the accessible system sizes to some hundred atoms, and routine DFT calculations are usually only done in this regime. Fortunately, it is still possible to reduce the cubic complexity of DFT calculation by using so-called linear scaling approaches [6,7], meaning that doubling the number of atoms in a system leads to a computation time that is only twice as large. The foundation of the linear scaling approaches lies in the locality of the density matrix $F(\mathbf{r}, \mathbf{r}')$. The so-called nearsightedness principle [8] states that the properties of the density matrix at a point $\mathbf{r}$ depend only on points $\mathbf{r}'$ in a localized region around $\mathbf{r}$, and indeed it can be shown that the matrix elements $F(\mathbf{r}, \mathbf{r}')$ decay exponentially with the distance $|\mathbf{r}-\mathbf{r}'|$ for insulators and metals at finite temperatures [9–13]. Since the density matrix is enough to completely describe a quantum mechanical system, this allows to eventually reach a DFT algorithm that scales linearly with system size.

* Corresponding author.
E-mail addresses: stephan.mohr@bsc.es (S. Mohr), luigi.genovese@cea.fr (L. Genovese).

https://doi.org/10.1016/j.nme.2018.01.002
Received 29 November 2017; Received in revised form 26 January 2018; Accepted 31 January 2018
Available online 14 February 2018

These theoretical foundations have given rise to a large variety of approaches to perform linear scaling DFT calculations [14–30]; an overview over linear scaling methods can be found in Refs. [6,7]. Together with the steadily increasing capacity of today's supercomputers, this has led to various DFT codes that exhibit such a linear scaling algorithm, as for instance ONETEP [31–34], CONQUEST [35–37], SIESTA [38], QUICKSTEP [39], OPENMX [40,41] or BIGDFT [42–44]; an overview of popular electronic structure codes and methods for large scale calculations can be found in Ref. [45].

However, these various implementations of linear scaling DFT are usually only applied to systems exhibiting a finite gap, and abundant demonstrations for metallic systems are missing. Still there are a few examples of reduced scaling methods for metals in the literature [46]. With respect to ONETEP, a recent implementation based on a direct free energy minimization technique allows to perform calculations for metallic systems, thereby reducing the computational workload [47]. In OPENMX, there is an implementation of a divide-and-conquer approach within a Krylov subspace that allows to perform linear scaling calculations for metals; however the method seems to require a careful tuning before it can be applied to large systems [41]. Furthermore it has been shown that the approach by Suryanarayana et al. [48], which calculates the electronic charge density and the total energy directly by performing Gauss quadratures over the spectrum of the Hamiltonian and in this way is capable to reach a linear complexity, also works for metallic systems [49]. Finally there also exist $\mathcal{O}(N)$ approaches related to Multiple Scattering Theory, such as the one based on the Korringa–Kohn–Rostoker (KKR) Green's-function method that showed linear scaling up to more than 16,000 atoms [50], and the locally self-consistent multiple scattering (LSMS) method [51], which in a recent GPU implementation has shown linear scaling up to 65,536 atoms [52].

These pioneering examples demonstrate that, even if their application is possible, reduced scaling approaches for large metallic systems have to be considered under a different perspective. As for such systems the number of degrees of freedom is very large and the electronic structure is complicated, first-principles calculation become a useful tool only when complementing other approaches, like for instance force fields, which are unable to provide quantum-mechanical information. When such kind of information is required, like for example when studying the arrangement of electrons close to a defective region, investigation techniques like the ones presented above are of utmost importance.

In this paper we report on the capabilities of BIGDFT to perform reduced and eventually also linear scaling calculations for a metallic system at finite temperature. Whereas previous publications have highlighted in detail the accuracy, efficiency and linear scaling capabilities of this code for systems with a finite HOMO-LUMO gap [43,44], metals have so far not been considered. In this paper we demonstrate that the basic algorithm of BIGDFT remains stable also for systems with vanishing gap and thus allows to routinely perform accurate linear scaling calculation for large metallic systems without the need of additional adjustments. As specific example we have chosen Tungsten due to its relevance for finding safe and long-lasting materials for fusion reactors. However we have also performed tests for other systems, and we see no obstacle in applying our method to other metals as well.

The outline of this paper is as follows: In Section 2 we focus on the theoretical background, with Section 2.1 summarizing the principles of the linear scaling version of BIGDFT, and Section 2.2 discussing how BIGDFT can mitigate the challenges arising for metallic systems. In Section 3 we then present numerical results, with Section 3.1 demonstrating the precision that we obtain with the linear scaling version of BIGDFT and Section 3.2 showing various performance figures.

2. Theory

2.1. Overview of the algorithm

The detailed implementation of the linear scaling algorithm of BIGDFT has been thoroughly presented in Refs. [43,44]. Here we will give a brief overview over the most important concepts.

The central quantity on which the algorithm is based, namely the density matrix, is represented in a separable way via a set of localized and adaptive basis functions $\{\phi_\alpha(\mathbf{r})\}$, from now on also called "support functions", as

$$F(\mathbf{r}, \mathbf{r}') = \sum_{\alpha,\beta} \phi_\alpha(\mathbf{r}) K^{\alpha\beta} \phi_\beta(\mathbf{r}'), \tag{1}$$

where the matrix $\mathbf{K}$ denotes the "density kernel". From this expression we can easily get the electronic charge density as $\rho(\mathbf{r}) = F(\mathbf{r}, \mathbf{r})$ and use it for the construction of the Kohn–Sham Hamiltonian,

$$\hat{\mathscr{H}}[\rho] = -\frac{1}{2}\nabla^2 + \hat{\mathscr{V}}_{KS}[\rho] + \hat{\mathscr{V}}_{PSP}, \tag{2}$$

where the Kohn–Sham potential $\hat{\mathscr{V}}_{KS}[\rho] = \int \frac{\rho(\mathbf{r}')}{|\mathbf{r}-\mathbf{r}'|} \mathrm{d}\mathbf{r}' + \hat{\mathscr{V}}_{XC}[\rho]$ contains the Hartree and exchange-correlation potential, and $\hat{\mathscr{V}}_{PSP}$ denotes the pseudopotential [53] that is used to describe the union of the nuclei and core electrons. This Hamiltonian operator gives rise to the Hamiltonian matrix $\mathbf{H}$, defined as

$$H_{\alpha\beta} = \int \phi_\alpha(\mathbf{r}) \hat{\mathscr{H}}(\mathbf{r}) \phi_\beta(\mathbf{r}) \mathrm{d}\mathbf{r}, \tag{3}$$

which can then be used to determine a new density kernel; methods to do so will be discussed later.

In order to obtain a linear scaling behavior, it is necessary to employ a set of *localized* support functions that eventually lead to sparse matrices. What distinguishes BIGDFT from other similar approaches is the special set of localized support functions that it uses. These are expanded in an underlying basis set of Daubechies wavelets [54] and are optimized in-situ. Daubechies wavelets offer the outstanding property of being at the same time orthogonal, systematic and exhibiting compact support; further details about the advantages of the usage of Daubechies wavelets can be found in Refs. [42,43]. The in-situ optimization, together with an imposed approximative orthonormality, results in a set of quasi-systematic support functions offering a very high precision. This allows to work with a *minimal* set of support functions, meaning that only very few functions per atom are necessary to obtain a very high accuracy. Obviously, this in-situ optimization comes at some cost compared to an approach working with a fixed set of non-optimized support functions. However, in the latter case we would require a much larger set to obtain the same precision [55], and all matrix operations in the subspace of the support functions, whose scaling is cubic in the worst case, would become considerably more costly. Apart from that, the use of a minimal basis set also has additional advantages, as for instance an easy and accurate fragment identification and associated population analysis for large systems [55], which can be used for a reliable effective electrostatic embedding [56].

2.2. Advantages of BIGDFT for metallic systems

DFT calculations for metallic systems are a challenging task. Due to the non-zero density of states at the Fermi energy, the occupation of the eigenstates around that energy value can easily jump between occupied and empty during the self-consistency cycle, leading to a phenomenon called "charge sloshing". A solution to this problem is to introduce a finite electronic temperature, leading to the grand-canonical extension of DFT as derived by Mermin [57]. In such a setup, the occupations are smoothed out around the Fermi level and the self-consistency cycle becomes more stable.

In the context of linear scaling approaches, the introduction of a

finite temperature has the additional advantage that it intensifies the decay properties of the density matrix, as mentioned in Section 1, and thus justifies the exploitation of the nearsightedness principle. Nevertheless, linear scaling calculations for metals remain very challenging. First of all, the used electronic temperatures must not be too large — otherwise one would change the physics in a too drastic way — and thus the density matrix decays much slower compared to finite gap systems. Moreover, the vanishing gap complicates the calculation of the density kernel. In BIGDFT, we use for this task the CHESS library [58] — one of the building-blocks of the BIGDFT program suite — that offers several different solvers. In the Fermi Operator Expansion (FOE) method [14,15], which is the linear scaling solver available within CHESS, one has to approximate the function that assigns the occupation numbers — typically the Fermi function — with Chebyshev polynomials. Obviously this method is most efficient if the degree of the polynomial expansion is small. This is the case if first the spectral width of the involved matrices is very small, and second if the Fermi function that must be approximated with the polynomials is smooth. Unfortunately the latter condition is violated for metals, since — even when using a small finite temperature — the Fermi function that must be approximated exhibits a sharp drop at the Fermi energy and we thus have to approximate a rather step-like function. As a consequence, it is questionable whether the FOE method can be used in practice for calculations with metals.

Fortunately it turns out that the special properties of the support functions used by BIGDFT lead to such a small spectral width that FOE can still be used for metallic systems. In Fig. 1 we show the density of states for the $9 \times 9 \times 9$ supercells (containing 1458 atoms) of body centered cubic (bcc) Tungsten (Fig. 1a) and Tantalum (Fig. 1b). As can be seen, the spectral width for Tungsten, the system on which we focus, is even smaller than the default $[-1, 1]$ interval for the Chebyshev polynomials. In this way the polynomial degree required to accurately represent the Fermi function can be kept reasonably small even for metallic systems.

The small spectral width is not a unique feature of Tungsten, as demonstrated by the plot for Tantalum. Rather it is a direct consequence of two central features of BIGDFT. First of all, the usage of pseudopotentials helps by eliminating the need for the treatment of core electrons whilst smoothening the behavior of the valence KS orbitals close to the nuclei. As an illustration we show in Fig. 2 the spectrum of the $9 \times 9 \times 9$ supercell of bcc Niobium, which was treated with a semicore pseudopotential (13 electrons). We see that, due to the presence of the semicore electrons, the spectral width is larger compared to Tungsten and Tantalum, which were treated with a pure valence pseudopotential (6 and 5 electrons, respectively). This directly translates into the polynomial degree used by the FOE method, which was of the order of 400–500 for Tungsten and Tantalum, but about 1200–1300 for Niobium. The second important point is the special way in which BIGDFT optimizes the support functions. As is explained in more detail in Ref. [43], a confining potential is used in order to properly localize the support functions during the optimization, and this confinement also seems to help in reducing the spectral width. In Fig. 3 we show the polynomial degree used by CHESS as function of the temperature for two sets of atomic orbitals. Both were obtained by solving the Schrödinger equation for the isolated atom within the pseudopotential approach, but in one case we additionally added the confining potential. In this latter setup, the resulting set of atomic orbitals exhibits a much smaller spectral width (36.7 eV) compared to the case without confinement (186.4 eV), leading to much smaller polynomial degrees.

Nevertheless it is important to note that FOE, even though it can be used very efficiently within BIGDFT, is an $\mathcal{O}(N)$ method designed for very large systems. For intermediate system size, alternative solvers within CHESS, such as diagonalization using LAPACK [59]/SCALAPACK [60] or PEXSI [61], might thus be more efficient. The first method does not exploit the sparsity of the matrices and thus exhibits a cubic scaling, whereas the second one scales as $\mathcal{O}(N)$, $\mathcal{O}(N^{3/2})$ and $\mathcal{O}(N^2)$ for one-, two- and three-dimensional systems, respectively. Still, FOE is the method of choice in the limit of very large systems since it is the only solver that scales strictly linearly with system size.

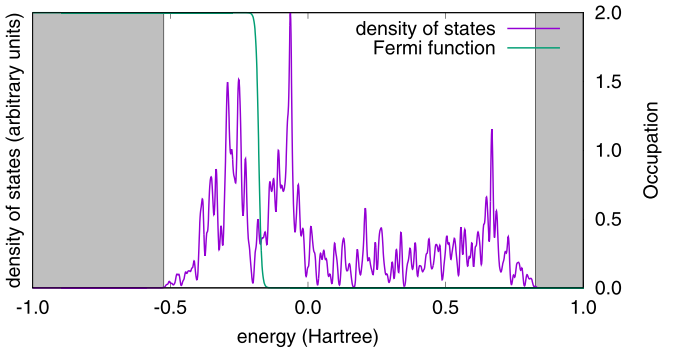

(a) Tungsten

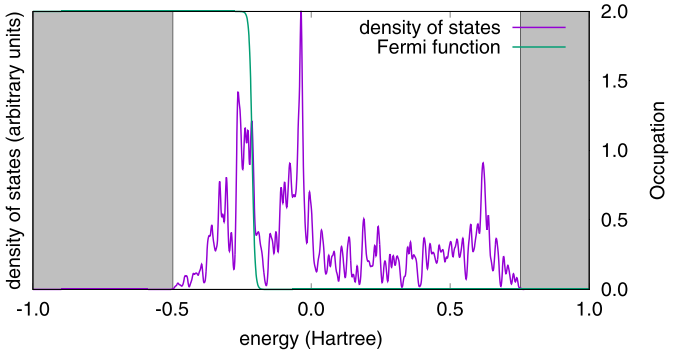

(b) Tantalum

Fig. 1. Density of states for the $9 \times 9 \times 9$ supercell (containing 1458 atoms) of bcc Tungsten and Tantalum. The spectral width is very small, which is a direct consequence of the usage of pseudopotentials and of the special properties of the support functions used by BIGDFT.

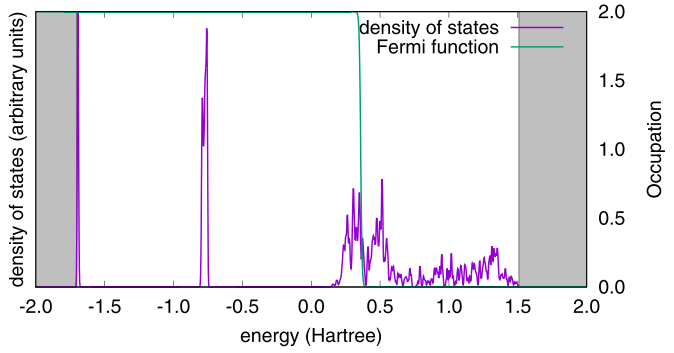

Fig. 2. Density of states for the $9 \times 9 \times 9$ supercell (containing 1458 atoms) of bcc Niobium. Compared to Fig. 1, the spectral width is larger due to the inclusion of semicore electrons.

3. Tests and considerations

In order to demonstrate the accuracy and performance of the linear scaling version of BIGDFT for metallic systems, we focus on one specific system, namely bcc Tungsten. All runs were performed using a grid spacing of at most 0.38 atomic units, the exchange-correlation part was described by the PBE functional [62], and the Krack HGH pseudopotential [63] was used. As we are interested in systems requiring the usage of very large supercells, we did not consider k-points in our calculations. Nevertheless, we still choose as test-bed for our approach a bulk-like system that can be easily simulated via k-points and small supercells, in order to verify the accuracy of our linear scaling

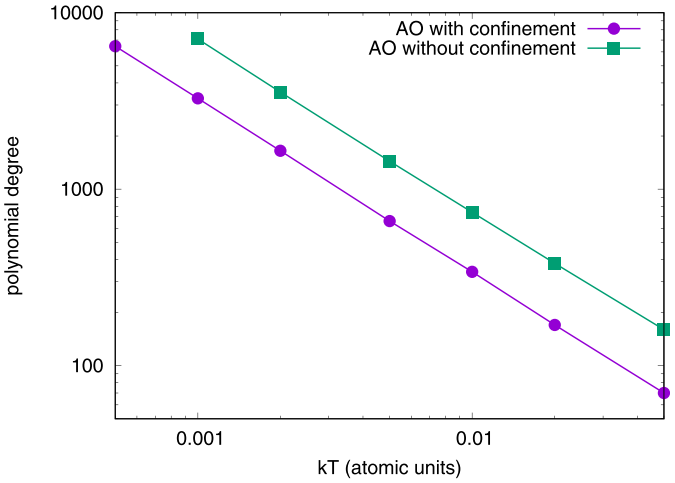

Fig. 3. Polynomial degree used by the FOE method within CHESS as a function of the electronic temperature, for two set of atomic orbitals (AO). The set that was obtained by solving the atomic Schrödinger equation with a confining potential leads to considerably lower values due to its smaller spectral width.

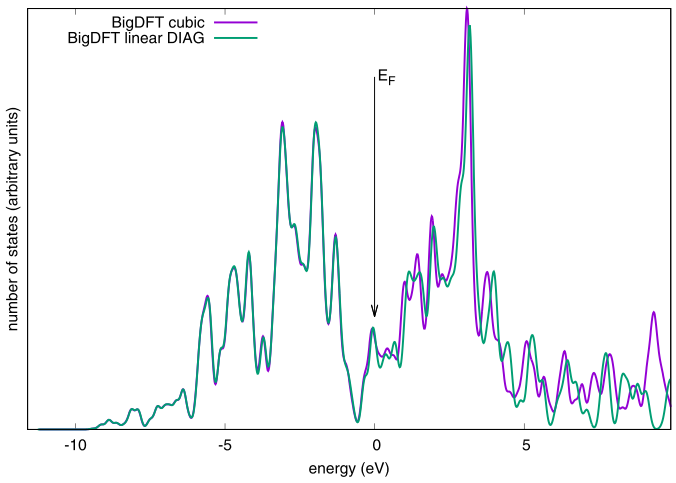

Fig. 5. Density of states for the cubic scaling version of BIGDFT and the linear scaling version with diagonalization. The energies were shifted such that the Fermi energy lies at zero. Up to the Fermi energy, the linear scaling version of BIGDFT yields results that are consistent with those of the traditional cubic scaling approach.

approach.

3.1. Accuracy of the linear scaling version

3.1.1. Energy versus volume

As a first test we demonstrate that the linear scaling version can accurately calculate the equation of state relating energy and volume. To this end, we scaled the lattice vectors of the Tungsten system by ± 4% around its equilibrium value. We compare four different setups: (1)/(2) the linear scaling version of BIGDFT using a 9 × 9 × 9 supercell (containing 1458 atoms) and no *k*-points, using as solver both diagonalization (DIAG) and FOE; (3) the cubic scaling version of BIGDFT using the 2-atoms unit cell and a 9 × 9 × 9 *k*-point mesh; (4) the same setup as (3), but run with the ABINIT code [64–67]. In Fig. 4 we compare the energy-vs-volume curves for all four setups. In the same figure we also show, for all four setups, the variation of the pressure as a function of the volume. As can bee seen from this test, the linear scaling approach correctly determines the optimal lattice parameter.

3.1.2. Density of states

As a second test we compare the density of states (DoS) in order to verify that the electronic structure is correctly described. In Fig. 5 we compare the DoS of the reference calculation with the cubic version of BIGDFT and the one obtained with the linear version with diagonalization. As can be seen, both setups yield an identical DoS for the occupied states. For the unoccupied ones, the linear version of BIGDFT shows some deviations. However, this is not surprising, since the optimization of the support functions only takes into account the occupied states, and a good accuracy can thus only be expected for the latter. However, as shown in Ref. [68] it is possible to include extra states in the optimization of the support functions in case that the user is interested in low-energy conduction states. Overall, we see that, thanks to the in-situ optimization of the support functions, the linear scaling version of BIGDFT is able to correctly reproduce the electronic structure of a metallic system.

3.2. Performance

3.2.1. Scaling with system size

As anticipated, we expect that DFT calculations of metallic systems at large scales will be time-consuming compared to similar simulations for insulators. In Fig. 6 we show the total runtime as a function of the number of atoms in the system, going from the 4 × 4 × 4 supercell (128 atoms) up to the 12 × 12 × 12 supercell (3456 atoms). As can be

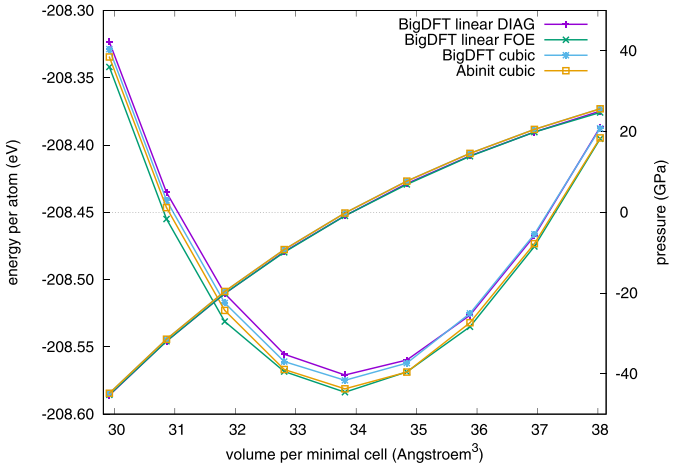

Fig. 4. Plots of the energy (left axis) and the pressure (right axis) as a function of the cell volume, for the four setups described in Section 3.1.1. The linear scaling version of BIGDFT yields results that are consistent with those of the two traditional cubic scaling approaches.

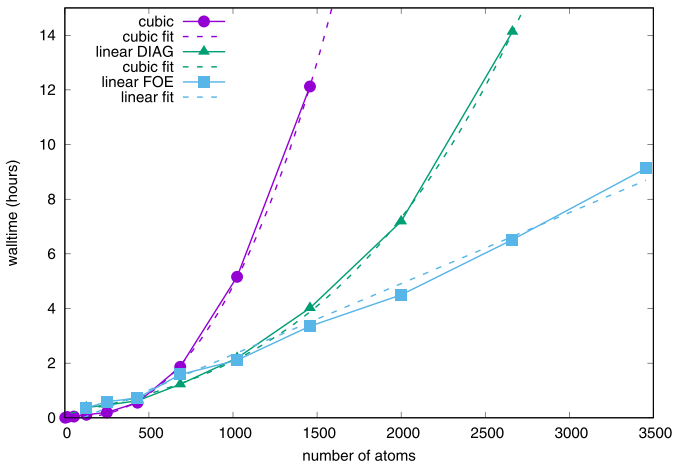

Fig. 6. Scaling of the total runtime as a function of the system size, for the cubic approach, the linear approach with diagonalization, and the linear approach with FOE. The calculations were performed at the Γ point, and the runs were performed in parallel, using 9600 cores (800 MPI tasks with 12 OpenMP threads).

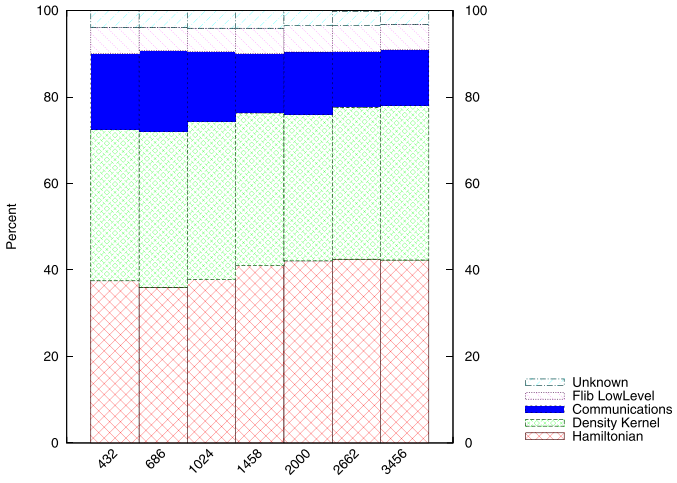

Fig. 7. Portions of the overall walltime spent in the different sections of the code for some of the FOE runs of Fig. 6. The overall behavior of the code is similar over a wide range of system sizes, indicated by the number of atoms on the *x*-axis. The FOE operations to construct the density kernel take a little less than 40% of the overall walltime.

seen, each of the three approaches that we compare — cubic, linear with diagonalization and linear with FOE — is characterized by a typical system size at which the method outperforms the other ones. For the small systems, the cubic approach is clearly the fastest one. Above about 500 atoms, the linear approach using diagonalization becomes the method of choice, since the cubic scaling of the diagonalization exhibits a rather small prefactor. For system sizes beyond about 1000 atoms, however, this cubic scaling starts to become a dominant part, and thus the truly linear scaling approach with FOE becomes the fastest option.

3.2.2. Considerations about the computational cost

We have demonstrated that the linear scaling version of BIGDFT can offer an unbiased and unconstrained description of metallic systems and is thus capable of yielding results that are of the same quality as those of a traditional cubic scaling approach. However, the inspection of the overall walltime clearly shows that the application to metals is much heavier compared to insulators. Considering the CPU-minutes per atom, which can be used as a metric to quantify the computational workload for $\mathcal{O}(N)$ codes [44], and comparing with values obtained for systems such as organic molecules of light atoms, reveals that the latter run up to two order of magnitude faster (!) on the same platform.

Nonetheless, this behavior is not related to the absence of a gap, but is due to the unbiased nature of the description, which requires support functions optimized *in-situ*. The reasons for this claim are explained in the following. In Fig. 7 we show the percentage of the time spent in the different sections of the code for the FOE runs of Fig. 6. We see that about 40% of the time is spent in the application of the KS Hamiltonian, 40% in the determination of the density matrix and some 20% in communications, and this over a wide range of number of atoms. All these calculations converged in about 15 iterations of the combined self-consistent optimization of the support functions and the density kernel. This fact shows, on the one hand, that FOE calculations of the kernel are not necessarily a bottleneck, even when higher polynomial degrees are needed, i.e. systems without a gap can be calculated efficiently with our method. On the other hand, it will be of much interest to work with *pre-optimized* basis functions that exhibit a similar accuracy, in the same spirit as the fragment-based approach that has been employed using molecular fragments with BigDFT [68,69]; this would provide results in only one (instead of 15) iterations and therefore lead to calculations running more than one order of magnitude faster. Work is ongoing in this direction.

4. Conclusions and outlook

In this work we have demonstrated, by applying our code BIGDFT to the case of large Tungsten systems, that it is possible to perform accurate and efficient linear scaling DFT calculations for metals with this code. We focused on Tungsten due to its relevance to Fusion, but an extension to other metals should not pose major obstacles thanks to the special features of BIGDFT. Even though the linear scaling version of this code was designed — as most other codes — for insulating systems, the obtained performance — considering also the very high accuracy of the resulting description — for metallic systems is excellent. We have shown that the results obtained with the linear scaling version of BIGDFT are of equal quality as those obtained with traditional cubic scaling approaches, but the reduced scaling allows to tackle much larger systems. The crossover point between the cubic and linear scaling treatment lies at about 500 atoms.

Thanks to these achievements, the possibility of addressing the challenge of unbiased first-principles investigations for systems with such a large degree of complexity opens up new interesting opportunities, as now more realistic conditions, like for instance lower concentrations of supercell defects, can be considered. Nevertheless it has to be pointed out that, despite the very good performance offered by our approach, calculations like the one presented remain extremely challenging from a first-principles point of view. Therefore, fully exploiting the potentialities of quantum-mechanical investigations of metallic systems at such sizes will only be possible if these investigations are considered as *complementary* techniques alongside other approaches at this scale.

Acknowledgments

We acknowledge valuable discussions with María José Caturla and Chu-Chun Fu. S.M. acknowledges support from the MaX project, which has received funding from the European Union's Horizon 2020 Research and Innovation Programme under Grant agreements 676598. M.A. acknowledges support from the Novartis Universität Basel Excellence Scholarship for Life Sciences and the Swiss National Science Foundation (P300P2-158407, P300P2-174475). We gratefully acknowledge the computing resources on Marconi-Fusion under the EUROfusion project BigDFT4F, from the Swiss National Supercomputing Center in Lugano (project s700), the Extreme Science and Engineering Discovery Environment (XSEDE) (which is supported by National Science Foundation grant number OCI-1053575), the Bridges system at the Pittsburgh Supercomputing Center (PSC) (which is supported by NSF award number ACI-1445606), the Quest high performance computing facility at Northwestern University, and the National Energy Research Scientific Computing Center (DOE: DE-AC02-05CH11231).

References

[1] O.A. Waseem, H.J. Ryu, Tungsten-based composites for nuclear fusion applications, in: R.O.A. Rahman, H.E.-D. M. Saleh (Eds.), Nuclear Material Performance, InTech, Rijeka, 2016, , http://dx.doi.org/10.5772/62434.
[2] D. Nguyen-Manh, A.P. Horsfield, S.L. Dudarev, Self-interstitial atom defects in BCC transition metals: group-specific trends, Phys. Rev. B 73 (2006) 020101, http://dx.doi.org/10.1103/PhysRevB.73.020101.
[3] L. Ventelon, F. Willaime, C.-C. Fu, M. Heran, I. Ginoux, Ab initio investigation of radiation defects in tungsten: structure of self-interstitials and specificity of di-vacancies compared to other bcc transition metals, J. Nucl. Mater. 425 (1) (2012) 16–21. Microstructure Properties of Irradiated Materials. doi:10.1016/j.jnucmat.2011.08.024 .
[4] P. Hohenberg, W. Kohn, Inhomogeneous electron gas, Phys. Rev. 136 (1964) B864, http://dx.doi.org/10.1103/PhysRev.136.B864.
[5] W. Kohn, L.J. Sham, Self-consistent equations including exchange and correlation effects, Phys. Rev. 140 (1965) A1133, http://dx.doi.org/10.1103/PhysRev.140.A1133.
[6] S. Goedecker, Linear scaling electronic structure methods, Rev. Mod. Phys. 71 (4) (1999) 1085, http://dx.doi.org/10.1103/RevModPhys.71.1085.
[7] D.R. Bowler, T. Miyazaki, O(n) methods in electronic structure calculations, Rep.

Prog. Phys. 75 (3) (2012) 036503.
[8] W. Kohn, Density functional and density matrix method scaling linearly with the number of atoms, Phys. Rev. Lett. 76 (1996) 3168–3171, http://dx.doi.org/10.1103/PhysRevLett.76.3168.
[9] J.D. Cloizeaux, Energy bands and projection operators in a crystal: analytic and asymptotic properties, Phys. Rev. 135 (1964) A685–A697, http://dx.doi.org/10.1103/PhysRev.135.A685.
[10] W. Kohn, J.R. Onffroy, Wannier functions in a simple nonperiodic system, Phys. Rev. B 8 (1973) 2485–2495, http://dx.doi.org/10.1103/PhysRevB.8.2485.
[11] J.J. Rehr, W. Kohn, Wannier functions in crystals with surfaces, Phys. Rev. B 10 (1974) 448–455, http://dx.doi.org/10.1103/PhysRevB.10.448.
[12] S. Goedecker, Decay properties of the finite-temperature density matrix in metals, Phys. Rev. B 58 (1998) 3501–3502, http://dx.doi.org/10.1103/PhysRevB.58.3501.
[13] S. Ismail-Beigi, T.A. Arias, Locality of the density matrix in metals, semiconductors, and insulators, Phys. Rev. Lett. 82 (1999) 2127–2130, http://dx.doi.org/10.1103/PhysRevLett.82.2127.
[14] S. Goedecker, L. Colombo, Efficient linear scaling algorithm for tight-Binding molecular dynamics, Phys. Rev. Lett. 73 (1994) 122–125, http://dx.doi.org/10.1103/PhysRevLett.73.122.
[15] S. Goedecker, M. Teter, Tight-binding electronic-structure calculations and tight-binding molecular dynamics with localized orbitals, Phys. Rev. B 51 (1995) 9455–9464, http://dx.doi.org/10.1103/PhysRevB.51.9455.
[16] S. Goedecker, Low complexity algorithms for electronic structure calculations, J. Comput. Phys. 118 (2) (1995) 261–268, http://dx.doi.org/10.1006/jcph.1995.1097.
[17] O.F. Sankey, D.A. Drabold, A. Gibson, Projected random vectors and the recursion method in the electronic-structure problem, Phys. Rev. B 50 (1994) 1376–1381, http://dx.doi.org/10.1103/PhysRevB.50.1376.
[18] U. Stephan, D.A. Drabold, Order-*N* projection method for first-principles computations of electronic quantities and wannier functions, Phys. Rev. B 57 (1998) 6391–6407, http://dx.doi.org/10.1103/PhysRevB.57.6391.
[19] W. Yang, Direct calculation of electron density in density-functional theory, Phys. Rev. Lett. 66 (1991) 1438–1441, http://dx.doi.org/10.1103/PhysRevLett.66.1438.
[20] W. Yang, A local projection method for the linear combination of atomic orbital implementation of density-functional theory, J. Chem. Phys. 94 (2) (1991) 1208–1214, http://dx.doi.org/10.1063/1.460028.
[21] W. Yang, T.-S. Lee, A density-matrix divide-and-conquer approach for electronic structure calculations of large molecules, J. Chem. Phys. 103 (13) (1995) 5674–5678, http://dx.doi.org/10.1063/1.470549.
[22] X.-P. Li, R.W. Nunes, D. Vanderbilt, Density-matrix electronic-structure method with linear system-size scaling, Phys. Rev. B 47 (1993) 10891–10894, http://dx.doi.org/10.1103/PhysRevB.47.10891.
[23] R. McWeeny, Some recent advances in density matrix theory, Rev. Mod. Phys. 32 (1960) 335–369, http://dx.doi.org/10.1103/RevModPhys.32.335.
[24] F. Mauri, G. Galli, R. Car, Orbital formulation for electronic-structure calculations with linear system-size scaling, Phys. Rev. B 47 (1993) 9973–9976, http://dx.doi.org/10.1103/PhysRevB.47.9973.
[25] P. Ordejón, D.A. Drabold, M.P. Grumbach, R.M. Martin, Unconstrained minimization approach for electronic computations that scales linearly with system size, Phys. Rev. B 48 (1993) 14646–14649, http://dx.doi.org/10.1103/PhysRevB.48.14646.
[26] P. Ordejón, D.A. Drabold, R.M. Martin, M.P. Grumbach, Linear system-size scaling methods for electronic-structure calculations, Phys. Rev. B 51 (1995) 1456–1476, http://dx.doi.org/10.1103/PhysRevB.51.1456.
[27] F. Mauri, G. Galli, Electronic-structure calculations and molecular-dynamics simulations with linear system-size scaling, Phys. Rev. B 50 (1994) 4316–4326, http://dx.doi.org/10.1103/PhysRevB.50.4316.
[28] J. Kim, F. Mauri, G. Galli, Total-energy global optimizations using nonorthogonal localized orbitals, Phys. Rev. B 52 (1995) 1640–1648, http://dx.doi.org/10.1103/PhysRevB.52.1640.
[29] W. Hierse, E.B. Stechel, Order-*n* methods in self-consistent density-functional calculations, Phys. Rev. B 50 (1994) 17811–17819, http://dx.doi.org/10.1103/PhysRevB.50.17811.
[30] E. Hernández, M.J. Gillan, Self-consistent first-principles technique with linear scaling, Phys. Rev. B 51 (1995) 10157–10160, http://dx.doi.org/10.1103/PhysRevB.51.10157.
[31] C.-K. Skylaris, P.D. Haynes, A.A. Mostofi, M.C. Payne, Introducing onetep: linear-scaling density functional simulations on parallel computers, J. Chem. Phys. 122 (8) (2005), http://dx.doi.org/10.1063/1.1839852.
[32] P.D. Haynes, C.-K. Skylaris, A.A. Mostofi, M.C. Payne, Onetep: linear-scaling density-functional theory with local orbitals and plane waves, Phys. Status Solidi B 243 (11) (2006) 2489–2499, http://dx.doi.org/10.1002/pssb.200541457.
[33] A.A. Mostofi, P.D. Haynes, C.K. Skylaris, M.C. Payne, Onetep: linear-scaling density-functional theory with plane-waves, Mol. Simul. 33 (7) (2007) 551–555, http://dx.doi.org/10.1080/08927020600932801.
[34] C.-K. Skylaris, P.D. Haynes, A.A. Mostofi, M.C. Payne, Recent progress in linear-scaling density functional calculations with plane waves and pseudopotentials: the onetep code, J. Phys. 20 (6) (2008) 064209.
[35] D.R. Bowler, I.J. Bush, M.J. Gillan, Practical methods for ab initio calculations on thousands of atoms, Int. J. Quantum Chem. 77 (5) (2000) 831–842, http://dx.doi.org/10.1002/(SICI)1097-461X(2000)77:5<831::AID-QUA5>3.0.CO;2-G.
[36] D.R. Bowler, R. Choudhury, M.J. Gillan, T. Miyazaki, Recent progress with large-scale ab initio calculations: the conquest code, Phys. Status Solidi B 243 (5) (2006) 989–1000, http://dx.doi.org/10.1002/pssb.200541386.
[37] D.R. Bowler, T. Miyazaki, Calculations for millions of atoms with density functional theory: linear scaling shows its potential. J. Phys. 22 (7) (2010) 074207, http://dx.doi.org/10.1088/0953-8984/22/7/074207.
[38] J.M. Soler, E. Artacho, J.D. Gale, A. García, J. Junquera, P. Ordejón, D. Sánchez-Portal, The siesta method for ab initio order- n materials simulation, J. Phys. 14 (11) (2002) 2745.
[39] J. VandeVondele, M. Krack, F. Mohamed, M. Parrinello, T. Chassaing, J. Hutter, Quickstep: fast and accurate density functional calculations using a mixed gaussian and plane waves approach, Comput. Phys. Commun. 167 (2) (2005) 103–128, http://dx.doi.org/10.1016/j.cpc.2004.12.014.
[40] T. Ozaki, H. Kino, Efficient projector expansion for the ab initio lcao method, Phys. Rev. B 72 (2005) 045121, http://dx.doi.org/10.1103/PhysRevB.72.045121.
[41] T. Ozaki, O(n) krylov-subspace method for large-scale ab initio electronic structure calculations, Phys. Rev. B 74 (2006) 245101, http://dx.doi.org/10.1103/PhysRevB.74.245101.
[42] L. Genovese, A. Neelov, S. Goedecker, T. Deutsch, S.A. Ghasemi, A. Willand, D. Caliste, O. Zilberberg, M. Rayson, A. Bergman, R. Schneider, Daubechies wavelets as a basis set for density functional pseudopotential calculations. J. Chem. Phys. 129 (1) (2008) 014109, http://dx.doi.org/10.1063/1.2949547.
[43] S. Mohr, L.E. Ratcliff, P. Boulanger, L. Genovese, D. Caliste, T. Deutsch, S. Goedecker, Daubechies wavelets for linear scaling density functional theory, J. Chem. Phys. 140 (20) (2014) 204110, http://dx.doi.org/10.1063/1.4871876.
[44] S. Mohr, L.E. Ratcliff, L. Genovese, D. Caliste, P. Boulanger, S. Goedecker, T. Deutsch, Accurate and efficient linear scaling dft calculations with universal applicability, Phys. Chem. Chem. Phys. 17 (2015) 31360–31370, http://dx.doi.org/10.1039/C5CP00437C.
[45] L.E. Ratcliff, S. Mohr, G. Huhs, T. Deutsch, M. Masella, L. Genovese, Challenges in large scale quantum mechanical calculations, Wiley Interdiscip. Rev. Comput. Mol. Sci. 7 (1) (2017) e1290, http://dx.doi.org/10.1002/wcms.1290. E1290
[46] J. Aarons, M. Sarwar, D. Thompsett, C.-K. Skylaris, Perspective: methods for large-scale density functional calculations on metallic systems, J. Chem. Phys. 145 (22) (2016) 220901, http://dx.doi.org/10.1063/1.4972007.
[47] Á. Ruiz-Serrano, C.-K. Skylaris, A variational method for density functional theory calculations on metallic systems with thousands of atoms, J. Chem. Phys. 139 (5) (2013) 054107, http://dx.doi.org/10.1063/1.4817001.
[48] P. Suryanarayana, K. Bhattacharya, M. Ortiz, Coarse-graining kohnsham density functional theory, J. Mech. Phys. Solids 61 (1) (2013) 38–60, http://dx.doi.org/10.1016/j.jmps.2012.09.002.
[49] M. Ponga, P. Ariza, M. Ortiz, K. Bhattacharya, Linear Scaling DFT for Defects in Metals, Springer International Publishing, Cham, pp. 265–272. doi:10.1007/978-3-319-48237-8_35.
[50] A. Thiess, R. Zeller, M. Bolten, P.H. Dederichs, S. Blügel, Massively parallel density functional calculations for thousands of atoms: kkrnano, Phys. Rev. B 85 (2012) 235103, http://dx.doi.org/10.1103/PhysRevB.85.235103.
[51] Y. Wang, G.M. Stocks, W.A. Shelton, D.M.C. Nicholson, Z. Szotek, W.M. Temmerman, Order-n multiple scattering approach to electronic structure calculations, Phys. Rev. Lett. 75 (1995) 2867–2870, http://dx.doi.org/10.1103/PhysRevLett.75.2867.
[52] M. Eisenbach, J. Larkin, J. Lutjens, S. Rennich, J.H. Rogers, Gpu acceleration of the locally selfconsistent multiple scattering code for first principles calculation of the ground state and statistical physics of materials, Comput. Phys. Commun. 211 (2017) 2–7. High Performance Computing for Advanced Modeling and Simulation of Materials. doi:10.1016/j.cpc.2016.07.013 .
[53] A. Willand, Y.O. Kvashnin, L. Genovese, Á. Vázquez-Mayagoitia, A.K. Deb, A. Sadeghi, T. Deutsch, S. Goedecker, Norm-conserving pseudopotentials with chemical accuracy compared to all-electron calculations, J. Chem. Phys. 138 (10) (2013) 104109, http://dx.doi.org/10.1063/1.4793260.
[54] I. Daubechies, Ten Lectures on Wavelets, Society for Industrial and Applied Mathematics, Philadelphia, 1992.
[55] S. Mohr, M. Masella, L.E. Ratcliff, L. Genovese, Complexity reduction in large quantum systems: fragment identification and population analysis via a local optimized minimal basis, J. Chem. Theory Comput. 13 (9) (2017) 4079–4088. PMID: 28732165 . doi:10.1021/acs.jctc.7b00291 .
[56] S. Mohr, M. Masella, L. Ratcliff, L. Genovese (2017), in preparation.
[57] N.D. Mermin, Thermal properties of the inhomogeneous electron gas, Phys. Rev. 137 (1965) A1441–A1443, http://dx.doi.org/10.1103/PhysRev.137.A1441.
[58] S. Mohr, W. Dawson, M. Wagner, D. Caliste, T. Nakajima, L. Genovese, Efficient computation of sparse matrix functions for large-scale electronic structure calculations: the chess library, J. Chem. Theory Comput. 13 (10) (2017) 4684–4698. PMID: 28873312 . doi:10.1021/acs.jctc.7b00348 .
[59] E. Anderson, Z. Bai, C. Bischof, S. Blackford, J. Demmel, J. Dongarra, J. Du Croz, A. Greenbaum, S. Hammarling, A. McKenney, D. Sorensen, LAPACK Users' Guide, third ed., Society for Industrial and Applied Mathematics, Philadelphia, PA, 1999.
[60] L.S. Blackford, J. Choi, A. Cleary, E. D'Azevedo, J. Demmel, I. Dhillon, J. Dongarra, S. Hammarling, G. Henry, A. Petitet, K. Stanley, D. Walker, R.C. Whaley, ScaLAPACK Users' Guide, Society for Industrial and Applied Mathematics, Philadelphia, PA, 1997.
[61] L. Lin, M. Chen, C. Yang, L. He, Accelerating atomic orbital-based electronic structure calculation via pole expansion and selected inversion, J. Phys. 25 (29) (2013) 295501.
[62] J.P. Perdew, K. Burke, M. Ernzerhof, Generalized gradient approximation made simple, Phys. Rev. Lett. 77 (1996) 3865, http://dx.doi.org/10.1103/PhysRevLett.77.3865.
[63] M. Krack, Pseudopotentials for h to kr optimized for gradient-corrected exchange-correlation functionals, Theor. Chem. Acc. 114 (1) (2005) 145–152, http://dx.doi.org/10.1007/s00214-005-0655-y.
[64] X. Gonze, J.-M. Beuken, R. Caracas, F. Detraux, M. Fuchs, G.-M. Rignanese, L. Sindic, M. Verstraete, G. Zerah, F. Jollet, M. Torrent, A. Roy, M. Mikami,

P. Ghosez, J.-Y. Raty, D. Allan, First-principles computation of material properties: the {ABINIT} software project, Comput. Mater. Sci 25 (3) (2002) 478–492, http://dx.doi.org/10.1016/S0927-0256(02)00325-7.

[65] X. Gonze, G. Rignanese, M. Verstraete, J. Betiken, Y. Pouillon, R. Caracas, F. Jollet, M. Torrent, G. Zerah, M. Mikami, P. Ghosez, M. Veithen, J.-Y. Raty, V. Olevano, F. Bruneval, L. Reining, R. Godby, G. Onida, D. Hamann, D. Allan, A brief introduction to the abinit software package, Z. Kristallogr. 220 (2005) 558–562, http://dx.doi.org/10.1524/zkri.220.5.558.65066.

[66] X. Gonze, B. Amadon, P.-M. Anglade, J.-M. Beuken, F. Bottin, P. Boulanger, F. Bruneval, D. Caliste, R. Caracas, M. Ct;, T. Deutsch, L. Genovese, P. Ghosez, M. Giantomassi, S. Goedecker, D. Hamann, P. Hermet, F. Jollet, G. Jomard, S. Leroux, M. Mancini, S. Mazevet, M. Oliveira, G. Onida, Y. Pouillon, T. Rangel, G.-M. Rignanese, D. Sangalli, R. Shaltaf, M. Torrent, M. Verstraete, G. Zerah, J. Zwanziger, Abinit: first-principles approach to material and nanosystem properties, Comput. Phys. Commun. 180 (12) (2009) 2582–2615, http://dx.doi.org/10.1016/j.cpc.2009.07.007.

[67] X. Gonze, F. Jollet, F. Araujo, D. Adams, B. Amadon, T. Applencourt, C. Audouze, J.-M. Beuken, J. Bieder, A. Bokhanchuk, E. Bousquet, F. Bruneval, D. Caliste, M. Cote, F. Dahm, F. Pieve, M. Delaveau, M.G. ando B.Dorado, C. Espejo, G. Geneste, L. Genovese, A. Gerossier, M. Giantomassi, Y. Gillet, D.R. Hamann, L. He, G. Jomard, J. Janssen, S. Roux, A. Levitt, A. Lherbier, F. Liu, I. Lukacevic, A. Martin, C. Martins, M.J.T. Oliveira, S. Ponce, Y. Pouillon, T. Rangel, G.-M. Rignanese, A.H. Romero, B. Rousseau, O. Rubel, A.A. Shukri, M. Stankovski, M. Torrent, M. Setten, B. Troeye, M.J. Verstraete, D. Waroquier, J. Wiktor, B. Xue, A. Zhou, J.W. Zwanziger, Recent developments in the abinit software package, Comput. Phys. Commun. 205 (2016) 106, http://dx.doi.org/10.1016/j.cpc.2016.04.003.

[68] L.E. Ratcliff, L. Genovese, S. Mohr, T. Deutsch, Fragment approach to constrained density functional theory calculations using daubechies wavelets, J. Chem. Phys. 142 (23) (2015) 234105, http://dx.doi.org/10.1063/1.4922378.

[69] L.E. Ratcliff, L. Grisanti, L. Genovese, T. Deutsch, T. Neumann, D. Danilov, W. Wenzel, D. Beljonne, J. Cornil, Toward fast and accurate evaluation of charge on-site energies and transfer integrals in supramolecular architectures using linear constrained density functional theory (CDFT)-based methods, J. Chem. Theory Comput. 11 (5) (2015) 2077–2086, http://dx.doi.org/10.1021/acs.jctc.5b00057.